APPLIED ORGANOMETALLIC CHEMISTRY, VOL. 11, 783–796 (1997)

# Surfactant Stabilized Palladium Colloids as Precursors for *cis*-Selective Alkyne-hydrogenation Catalysts†

H. Bönnemann,[1]* W. Brijoux,[1] K. Siepen,[1] J. Hormes,[2] R. Franke,[2] J. Pollmann[2] and J. Rothe[2]

[1] Max-Planck-Institut für Kohlenforschung, Kaiser-Wilhelm-Platz 1, D-45466 Mülheim an der Ruhr, Germany

[2] Physikalisches Institut der Universität Bonn, Nußallee 12, D-53115 Bonn, Germany

**The performance of heterogeneous catalysts based on surfactant-stabilized palladium colloids is compared with conventional Pd/C and Lindlar catalysts in the partial hydrogenation of 3-hexyn-1-ol under optimized reaction conditions. The selectivity can be influenced by the protective shell as well as by the support and various promoters. The zwitterionic surfactant sulfobetaine-12 (*N*,*N*-dimethyl-dodecylammoniopropanesulfonate) appears to be best suited as a protective shell for highly selective palladium-colloid catalysts under the surfactants tested. The preferred support is $CaCO_3$: the Pd(SB12) colloids supported on $CaCO_3$ show the highest selectivities and activities of all tested catalysts. The best selectivity (98.1%) towards the desired *cis*-3-hexen-1-ol (leaf alcohol) is obtained with a lead-promoted palladium colloid supported on $CaCO_3$. This catalyst is slightly (0.5%) better in selectivity and twice as active as a conventional Lindlar catalyst. © 1997 John Wiley & Sons, Ltd.**

*Appl. Organometal. Chem.* **11**, 783–796 (1997)

No. of Figures: 21 No. of Tables: 5 No. of Refs: 15

**Keywords: metal colloids; palladium; Lindlar catalysts; catalysis; hydrogenation; leaf alcohol; XPS; XANES; TEM/EDX**

*Received 7 November 1996; accepted 16 January 1997*

* Correspondence to: H. Bönnemann.

† Dedicated to Professor Günter Schmid, Essen University, Germany, on the occasion of his 60th birthday on 22 January 1997.

Contract grant sponsor: BMBF; Contract grant number: FKZ 03 D0007 A2.

## INTRODUCTION

The *cis*-product of the partial hydrogenation of 3-hexyn-1-ol, leaf alcohol, is used as a fragrance with an annual production, estimated in 1996, of approx. 400 tonnes per annum (including esters):[1]

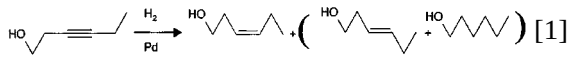

[1]

The use of heterogeneous palladium (Pd) catalysts for selective hydrogenations has been known since 1930.[2,3] In 1952, Lindlar[4] reported that refluxing of $Pd/CaCO_3$ catalysts in an aqueous solution of $Pb(acetate)_2$ increases the selectivity for the hydrogenation of alkynes to *cis*-alkenes. Various promoters such as chinoline, ethylenediamine or carbon monoxide (CO) raise the selectivity additionally, mainly by suppression of side reactions. The influence of lead (Pb) on the morphology of a $Pd/CaCO_3/Pb$ catalyst has been investigated by Maier and co-workers.[5] Lead promotion was found to increase the Pd particle size. Palczewska *et al.*[6] have reported that a $Pd_3Pb$ alloy catalyst has a higher selectivity in the gas-phase hydrogenation of acetylenes to the alkene than a conventional Lindlar catalyst. Evidence for the formation of a $Pd_3Pb$ phase was obtained by X-ray diffraction (XRD), X-ray photoelectron spectroscopy (XPS) and hydrogen chemisorption.

In the case of a colloidal Pd precursor, the protective shell, the support and the composition of bimetallic particles can be varied over a wide range. This paper describes the application of surfactant-stabilized Pd colloids in the partial hydrogenation of 3-hexyn-1-ol. In addition, the performance of the different colloid catalysts has been tested with an industrial standard test reaction (the hydrogenation of cinnamic acid).

 CCC 0268–2605/97/100783–14 $17.50

The influence of the protective shell, the support and various promoters on the catalytic properties is reported.

The interaction between the metal and the protecting shell has been investigated by X-ray absorption near-edge structure (XANES) and XPS, and the dispersity of the metal by CO chemisorption. Additional IR investigations of chemisorbed CO have also been undertaken. The morphology and particle composition have been investigated by transmission electron microscopy/energy dispersive X-ray spectroscopy (TEM/EDX). The characterization of the chemical state of the as-prepared and supported Pd colloids was carried out by means of X-ray photoelectron spectroscopy (XPS) and XANES.

## EXPERIMENTAL

### Preparation of the colloids

The preparation of $NR_4^+$-stabilized Pd colloids has been described elsewhere.[7] $Pd[NR_4^+]$ colloids have been prepared by reducing $PdCl_2$ with $NR_4B(ethyl)_3H$ in tetrahydrofuran (THF) (strategy 1) or by reducing $Pd[NR_4]_2Cl_2Br_2$ with $LiB(ethyl)_3H$ in THF (strategy 2).

### Pd[$NR_4$] (5% wt) charcoal catalyst

The dried colloid (1 mmol Pd) was dispersed in THF and added dropwise to a suspension of 2.0 g (5% wt) coverage) charcoal (Degussa support 101, batch no. 514) over 16 h. The colorless

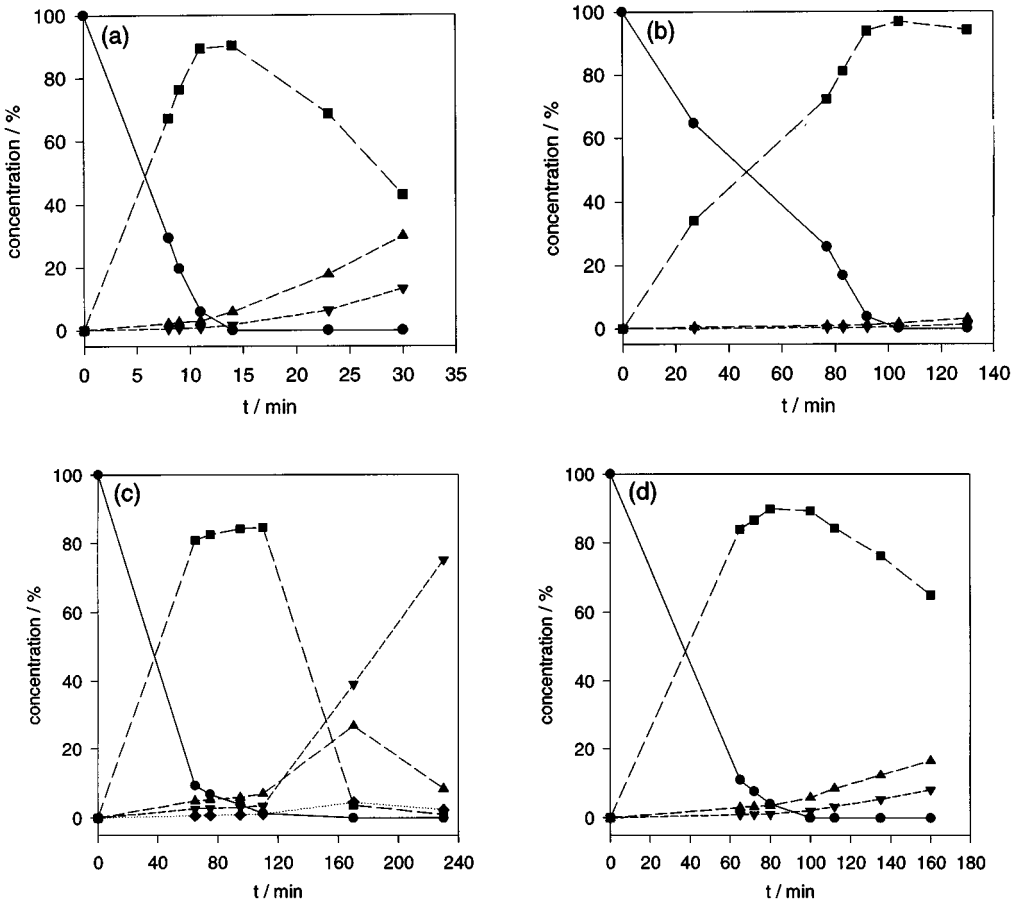


**Figure 1** Reaction profiles of (a) 5% wt. Pd/charcoal industrial catalyst (E105 XR/D Degussa AG), (b) 5% wt. Pd + 3.5% wt. Pb/$CaCO_3$ industrial catalyst (CE 407 R/D Degussa AG), (c) $Pd[N(octyl)_4]$/charcoal colloidal catalyst and (d) Pd(SB12)/charcoal colloidal catalyst in the *cis*-selective hydrogenation of 3-hexyn-1-ol. ●, 3-Hexyn-1-ol; ■, *cis*-3-hexen-1-ol; ▲ *trans*-3-hexen-1-ol; ▼, hexanol.

 

dispersion was filtered off through a D4 glass frit and the catalyst dried *in vacuo* ($10^{-3}$ mbar) for 16 h at room temperature. The catalyst can be handled in air after drying in vacuum at 1 mbar for 16 h.

### SB12-stabilized Pd colloid

A suspension of 0.177 g (1 mmol) $PdCl_2$ and 0.67 g (2 mmol) SB12 in THF was reduced by adding dropwise a solution of 0.9 ml (1.4 mmol) 1.56 M $LiB(ethyl)_3H$ in THF over 16 h at room temperature. After adding 2 ml of absolute acetone, the reaction mixture was stirred for 1 h. The suspension of the grey–brown colloid in THF was allowed to settle over several hours. The supernatant solution was removed and after drying the gray powder *in vacuo* ($10^{-3}$ mbar) at room temperature, a water-soluble Pd colloid was isolated.

**Table 1** Partial hydrogenation of 3-hexyn-1-ol with industrial and colloidal Pd catalysts

| Catalyst | Reaction time[a] (min) | Selectivity for *cis*-3-hexen-1-ol(%)[a] |
|---|---|---|
| E 105 XR/D | 11 | 95.1 |
| CE 407 R/D | 92 | 97.6 |
| $Pd[N(octyl)_4]/C$ | 47 | 89.6 |
| Pd(SB12)/C | 80 | 94.4 |

[a] *ca* 100% conversion.

### Pd(SB12) (5% wt)/$CaCO_3$ catalyst

The dried Pd colloid was dispersed in deionized water. The brown colloidal dispersion was added dropwise to a suspension of $CaCO_3$ in deionized water. The catalyst was allowed to settle for several hours and the supernatant, a colorless aqueous phase, was removed. The colloid was dried *in vacuo* (1 mbar) after freezing in liquid nitrogen to prevent foaming. The light gray–brown catalyst can be handled in air.

### Pd(SB12) (5% wt)/$CaCO_3$/Pb (2% wt) catalyst

A suspension of 0.709 g (4 mmol) $PdCl_2$ and 1.88 g (5.6 mmol) SB12 in *ca* 200 ml absolute

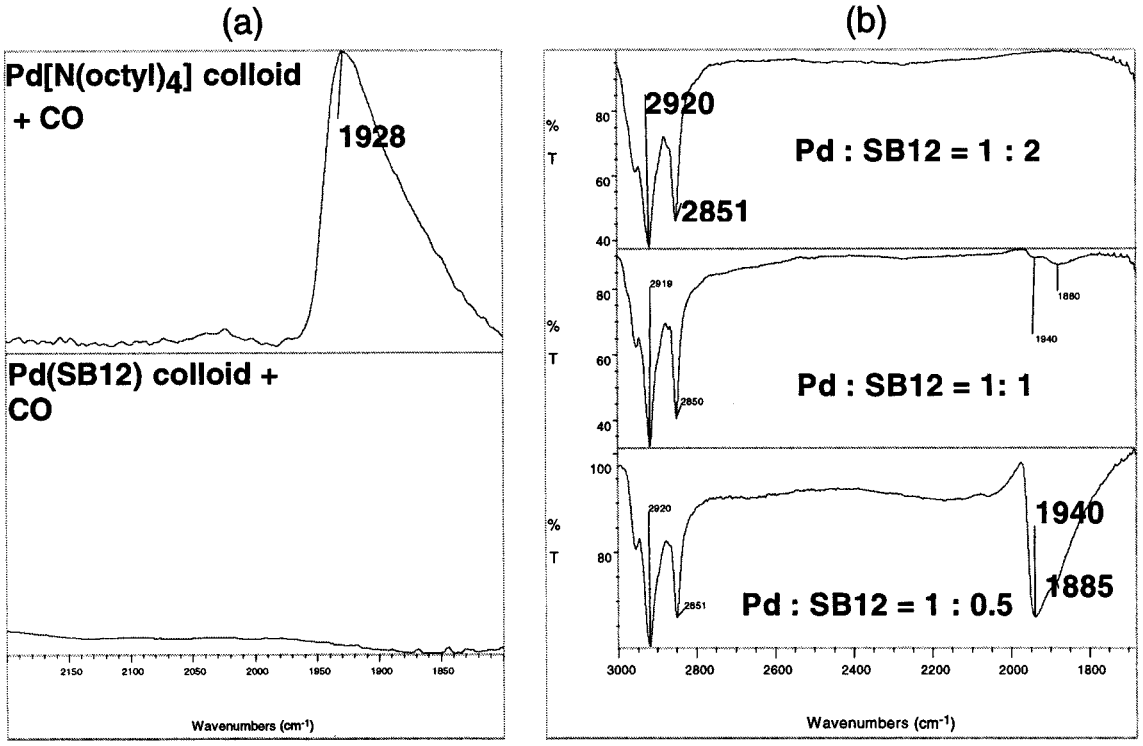


**Figure 2** (a) IR-spectra of CO-loaded $Pd[N(octyl)_4]$ and Pd(SB12) colloids; (b) IR-spectra of CO-loaded Pb(SB12)-colloids with different metal/SB12-ratios.

 

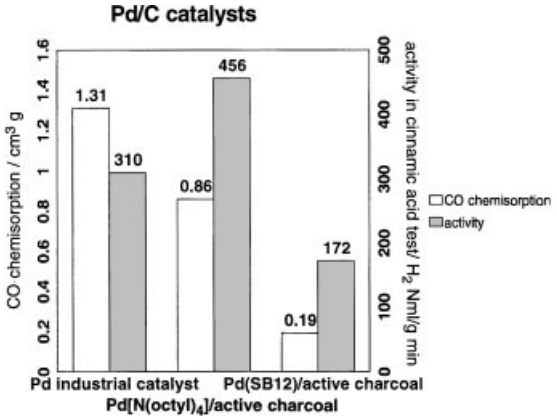


**Figure 3** Correlation of CO chemisorption and hydrogenation activity of Pd colloidal catalysts and a conventional Pd catalyst.

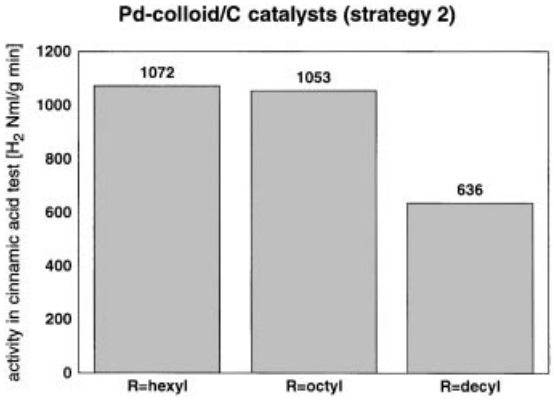


**Figure 4** Hydrogenation activity of Pd[$NR_4$]-colloid catalysts in the cinnamic acid test (R = hexyl, octyl, decyl).

**Table 2** Partial hydrogenation of 3-hexyn-1-ol with $NR_4$-stabilized Pd-colloid catalysts

| Catalyst | Reaction time[a] (min) | Selectivity for *cis*-3-hexen-1-ol(%)[a] |
|---|---|---|
| Pd[N(hexyl)$_4$]/C | 70 | 89.2 |
| Pd[N(octyl)$_4$]/C | 60 | 87.2 |
| Pd[N(decyl)$_4$]/C | 92 | 85.4 |

[a] *ca* 100% conversion.

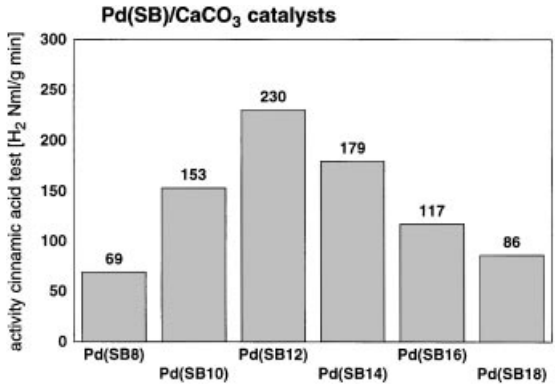


**Figure 5** Hydrogenation activity of Pd(SB*n*)-colloid catalysts in the cinnamic acid test (*n* = 8–18).

**Table 3** Partial hydrogenation of 3-hexyn-1-ol with SB-stabilized Pd colloid catalysts

| Catalyst | Reaction time[a] (min) | Selectivity for *cis*-3-hexen-1-ol(%)[a] |
|---|---|---|
| Pd(SB8)/$CaCO_3$ | 108 | 82 |
| Pd(SB10)/$CaCO_3$ | 27 | 94 |
| Pd(SB12)/$CaCO_3$ | 10 | 95 |
| Pd(SB14)/$CaCO_3$ | 31 | 91 |

[a] *ca* 100% conversion.

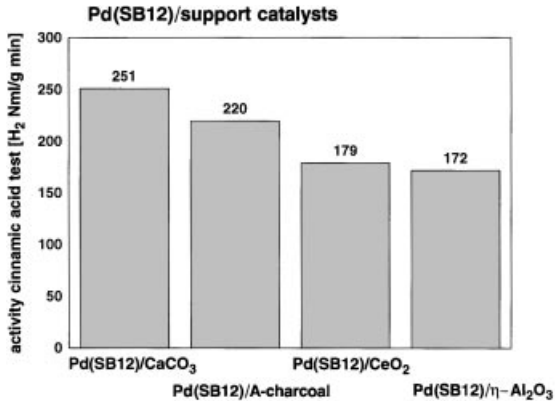


**Figure 6** Hydrogenation activity of Pd(SB12) colloids on different supports in the cinnamic acid test.

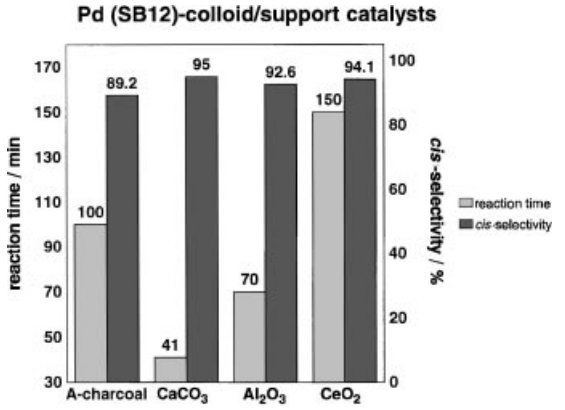


**Figure 7** Activity and *cis*-selectivity of Pd(SB12) colloids on different supports in the hydrogenation of 3-hexyn-1-ol.

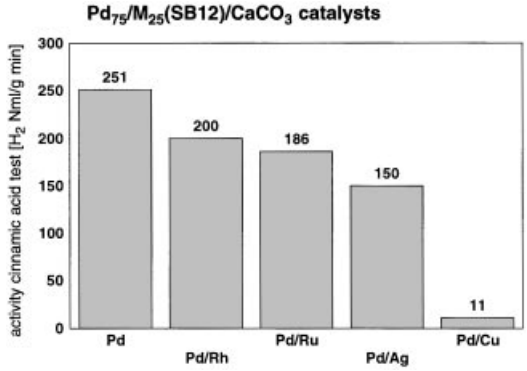


**Figure 8** Hydrogenation activity of Pd(SB12) colloid and bimetallic Pd/M colloids supported on $CaCO_3$ in the cinnamic acid test.

**Table 4** Partial hydrogenation of 3-hexyn-1-ol with SB12-stabilized Pd-colloid and bimetallic-colloid catalysts

| Catalyst $Pd_{75}/M_{25}$(SB12)/$CaCO_3$ | Reaction time[a] (min) | Selectivity for *cis*-3-hexen-1-ol (%)[a] |
|---|---|---|
| Pd | 41 | 95.3 |
| Pd/Rh | 44 | 93.1 |
| Pd/Ru | 25 | 94.3 |
| Pd/Ag | 22 | 92.9 |
| Pd/Zn | 22 | 92.9 |
| Pd/Cu | 210 | 95.7 |

[a] *ca* 100% conversion.

THF was reduced under argon by adding dropwise a solution of 3.6 ml (5.6 mmol) $LiB(ethyl)_3H$ in THF (1.5 M) diluted in 50 ml THF over 16 h. The colloid formed as a gray precipitate. The reaction mixture was stirred with 2 ml of absolute acetone and the solvent removed *in vacuo* ($10^{-3}$ mbar) at room temperature. The dried colloid was dispersed in 400 ml deionized water in air. A 100-ml portion of the colloidal dispersion was added to a suspension of 2.0 g $CaCO_3$ in water and refluxed with 75 mg Pb(acetate)$_2$ for 15 min. The gray–brown powder was allowed to settle and the clear supernatant aqueous phase was removed. The catalyst was dried at 90 °C for 6 h.

### $Pd_3Pb$(SB12)/$CaCO_3$ catalyst (5% wt Pd + 3.5% wt Pb)

$PdBr_2$ (0.200 g; 0.75 mmol), $PbBr_2$ (0.092 g; 0.25 mmol) and SB12 (0.67 g; 2 mmol) in *ca* 50 ml absolute THF were reduced under argon by adding dropwise a solution of 0.9 ml (1.4 mmol) $LiB(ethyl)_3H$ in THF (1.5 M) diluted in 50 ml THF over 16 h. The colloid formed as a gray precipitate. The reaction mixture was stirred with 2 ml of absolute acetone and the solvent removed *in vacuo* ($10^{-3}$ mbar) at room temperature. The dried colloid was dispersed in 100 ml deionized water in air and the colloidal dispersion was added to a suspension of 1.5 g $CaCO_3$ in water and refluxed with 75 mg Pb(acetate)$_2$ for 15 min. The gray–brown powder was allowed to settle and the clear supernatant aqueous phase was removed. The catalyst was dried at 90 °C for 6 h.

### Liquid-phase hydrogenation of cinnamic acid

The test procedure has been described elsewhere.[8]

### Liquid-phase hydrogenation of 3-hexyn-1-ol

All hydrogenation experiments were performed at 1 bar and −10 °C with a substrate (3-hexyn-1-ol) concentration of 0.4 mol $l^{-1}$, using 0.100 g of catalyst, and the reaction was stirred at 2000 rpm in 100 ml ethanol. Before adding the substrate, the reaction mixture was allowed to temper at −10 °C. After the uptake of *ca* 80% of the calculated hydrogen volume, 6–10 0.1 ml

 

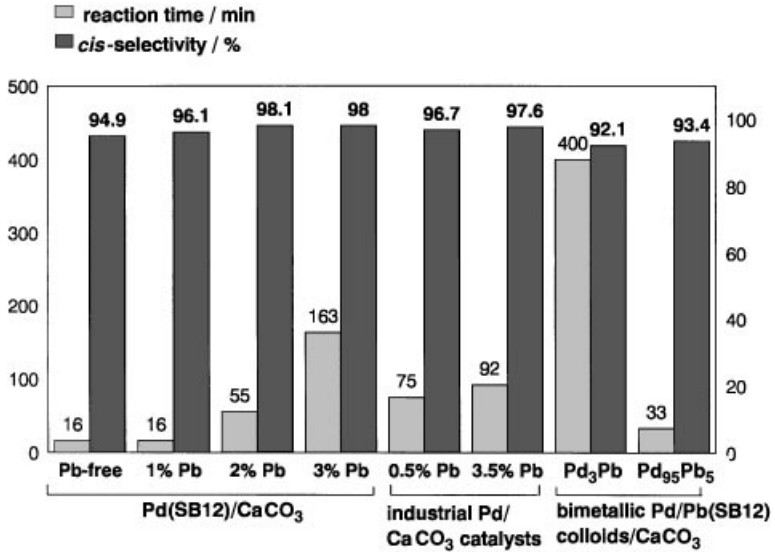


**Figure 9** Activity and *cis*-selectivity of Pd-colloid catalysts in the hydrogenation of 3-hexyn-1-ol compared with conventional Lindlar catalysts, and the influence of lead poisoning.

GC samples were taken at short intervals until complete conversion had occurred.

### Instrumentation

CO chemisorption measurements were carried out using a Micromeritics ASAP 2000 chemisorption system. Catalyst (0.2–0.3 g) was weighed into a U-shaped quartz glass tube and degassed at 150 °C and $10^{-6}$ mbar for 16 h. After this pretreatment, the sample was evacuated and reduced *in situ* in a hydrogen stream at 40 °C for 1 h. The hydrogen was removed from the metal surface by heating the sample at 90 °C and $10^{-6}$ mbar. The CO chemisorption was carried out at 35 °C and the physically adsorbed CO removed by evacuating the sample at 35 °C for 30 min, followed by repeated CO adsorption. The last step represents the physisorbed CO volume which is subtracted to give the chemisorbed CO.

High-resolution TEM micrographs were obtained with a Hitachi HF2000 microscope at 200 kV. EDX analysis was measured with an NORAN spectrometer connected to the microscope. TEM micrographs of a thin section of the $Pd_3Pb(SB12)/CaCO_3$ catalyst were kindly provided by Degussa AG.

XANES spectra were measured on the BN3 beamline of the synchrotron radiation laboratory at the Electron Stretcher and Accelerator (ELSA) of Bonn University (Germany). The data were evaluated with Bertagnolli software (V13).[9] XPS spectra were recorded with a VG Instruments CLAM2 electron energy analyzer working in the constant-pass mode (50 eV) under irradiation with Al-K$\alpha$ radiation from an X-ray tube. Sample charge correction was performed using the C1s signal (280.0 eV) originating from hydrocarbons present in the protecting shell.

IR spectra were recorded with Bruker IFS 48 and Nicolet 7199 FT-IR spectrometers. The samples were measured between two KBr plates or as KBr pressings.

## RESULTS AND DISCUSSION

The influence of the protective shell round the Pd colloidal catalysts on the selectivity of the partial hydrogenation of 3-hexyn-1-ol and the activity in the cinnamic acid test was found to be significant. The type of surfactant (cationic or zwitterionic), as well as the chain length of the lipophilic alkyl chains in the surfactant, influences the catalytic properties. In the case of the partial hydrogenation of 3-hexyn-1-ol, the colloid stabilized with the zwitterionic sulfobetaine showed higher selectivities than the tetra-alkylammonium cationic surfactant (Fig. 1; Table 1).

CO chemisorption on the Pd(SB12)-colloid catalyst is four times lower than on the charcoal-supported $Pd[N(octyl)_4]$-colloid catalyst.

 

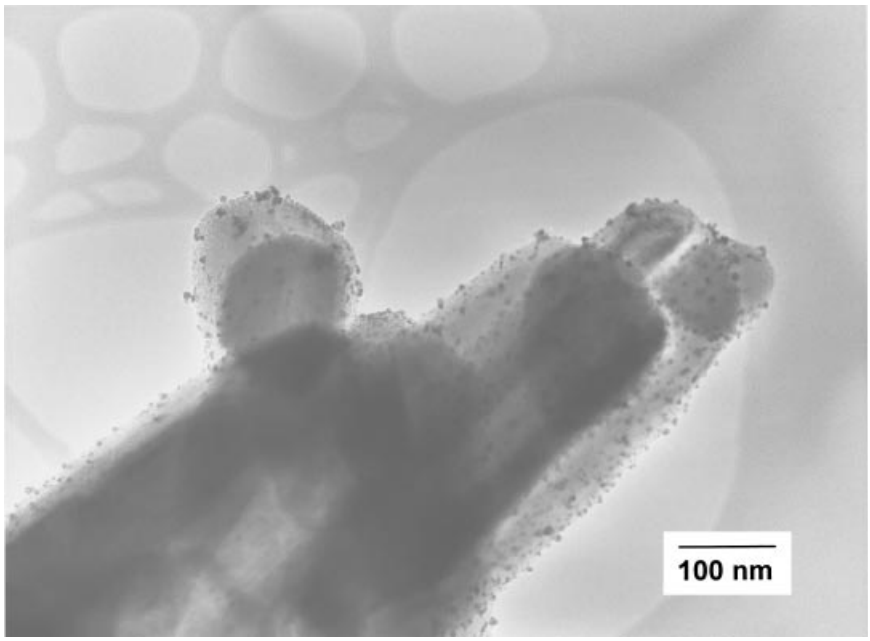


**Figure 10** TEM of $Pd_3Pb(SB12)/CaCO_3$ catalyst.

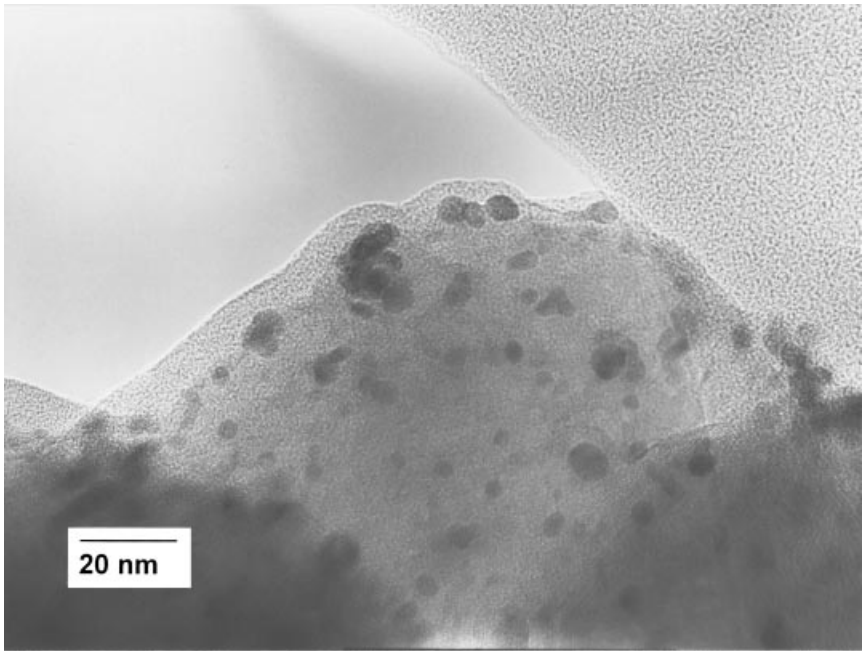


**Figure 11** High-resolution TEM of $Pd_3Pb(SB12)/CaCO_3$ catalyst.

 

Coordination of CO to the Pd surface has been investigated by IR spectroscopy (Fig. 2). Both colloids show only a single band typical for double-bridged CO. In the case of the Pd(SB12) colloid, the band could only be observed when the Pd/SB12 ratio was reduced to 1:0.5. A linear Pd–CO absorption band was not observed, since this species is desorbed when the solvent is evaporated.

The number of accessible surface Pd atoms is significantly lower when SB12 is used as a protective shell. This results from most of the particle surface being covered by SB12 molecules and correlates well with the hydrogenation activities in the cinnamic acid test (Fig. 3). In the hydrogenation of cinnamic acid the activity of the Pd(SB12)/charcoal catalyst is lower than that of the Pd[N(octyl)$_4$]/charcoal catalyst (colloid prepared by strategy 1), which shows an activity of *ca* 456 ml g$^{-1}$ min$^{-1}$ (STP). The CO chemisorption results show that in the case of the colloidal catalysts the metal surface is covered by the protective shell to a different extent. The number of accessible surface atoms, represented by the chemisorbed CO volume, is much lower for Pd colloids stabilized by SB12 than by N(octyl)$_4^+$. This is caused by the larger particle size of the SB12-stabilized colloid medium (5 nm) compared with the $NR_4^+$-stabilized colloid (2 nm) as well as by the steric requirements of the surfactant adsorbed on the particle surface. The industrial catalyst consists of uncovered particles and exhibits the highest CO chemisorption but not the highest activity.

The length of the alkyl chains in the $NR_4^+$-stabilized Pd-colloid catalysts influences the hydrogenation activity in the cinnamic acid test (Fig. 4): the longer the chains, the lower the hydrogenation activity. This result is in agreement with those found for $NR_4^+$-stabilized Pt- and Rh-colloid catalysts and the CO chemisorption results,[10] which show that the accessible surface area on the metal decreases with increasing alkyl chain length.

In the partial hydrogenation of 3-hexyn-1-ol, the alkyl chain length also influences the selectivity (Table 2), which is found to decrease with increasing chain length.

In the case of catalysts based on sulfobetaine-stabilized Pd colloids, the influence of the length of the alkyl chains on the hydrogenation activity in the cinnamic acid test was as follows:

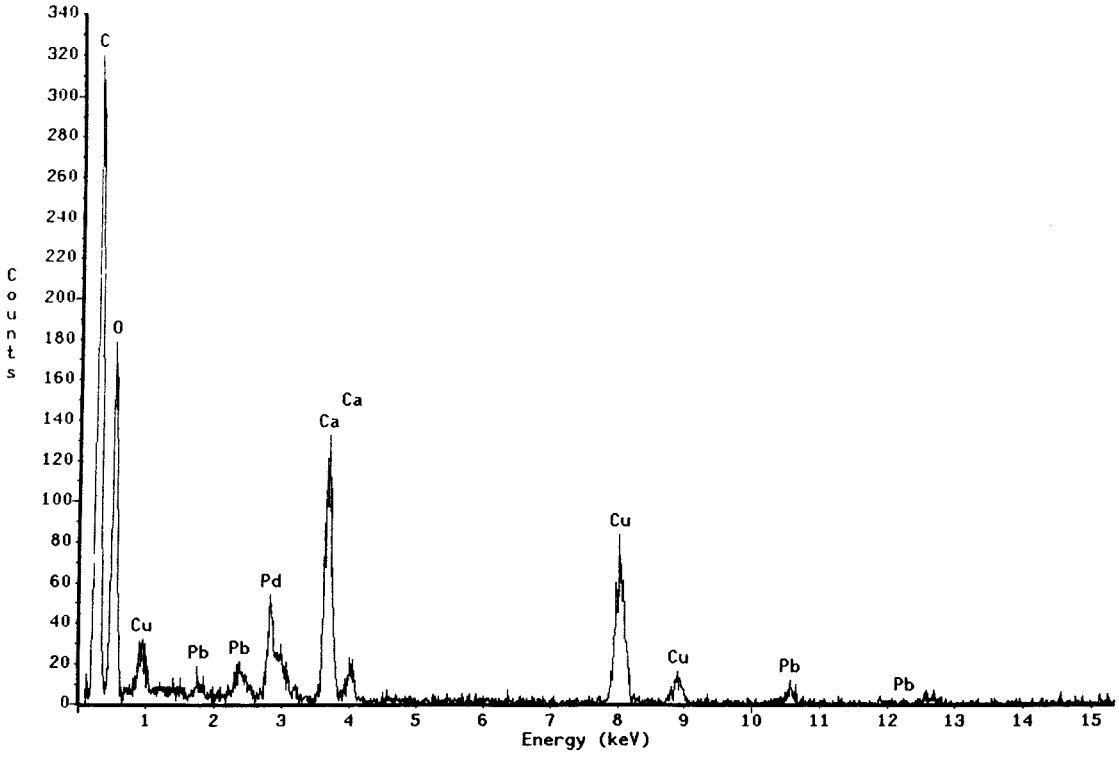


**Figure 12** EDX of $Pd_3Pb$(SB12)/$CaCO_3$ catalyst.

 

increasing the chain length in steps of $C_2$ units from octyl to dodecyl was accompanied by an increase in activity, while any further increase in the chain length from dodecyl to octadecyl resulted in a decrease (Fig. 5).

This finding correlates satisfactorily with the selectivity of these catalysts for the partial hydrogenation of 3-hexyn-1-ol (Table 3). The Pd(SB10)/$CaCO_3$ and Pd(SB12)/$CaCO_3$ catalysts showed the highest selectivities. In this case, the low selectivity of the SB8-stabilized Pd-colloid may well have been a result of the unfavorable stabilization properties of this surfactant which led to the formation of large, unselective Pd particles. As a result, this catalyst showed lower activities in both reactions.

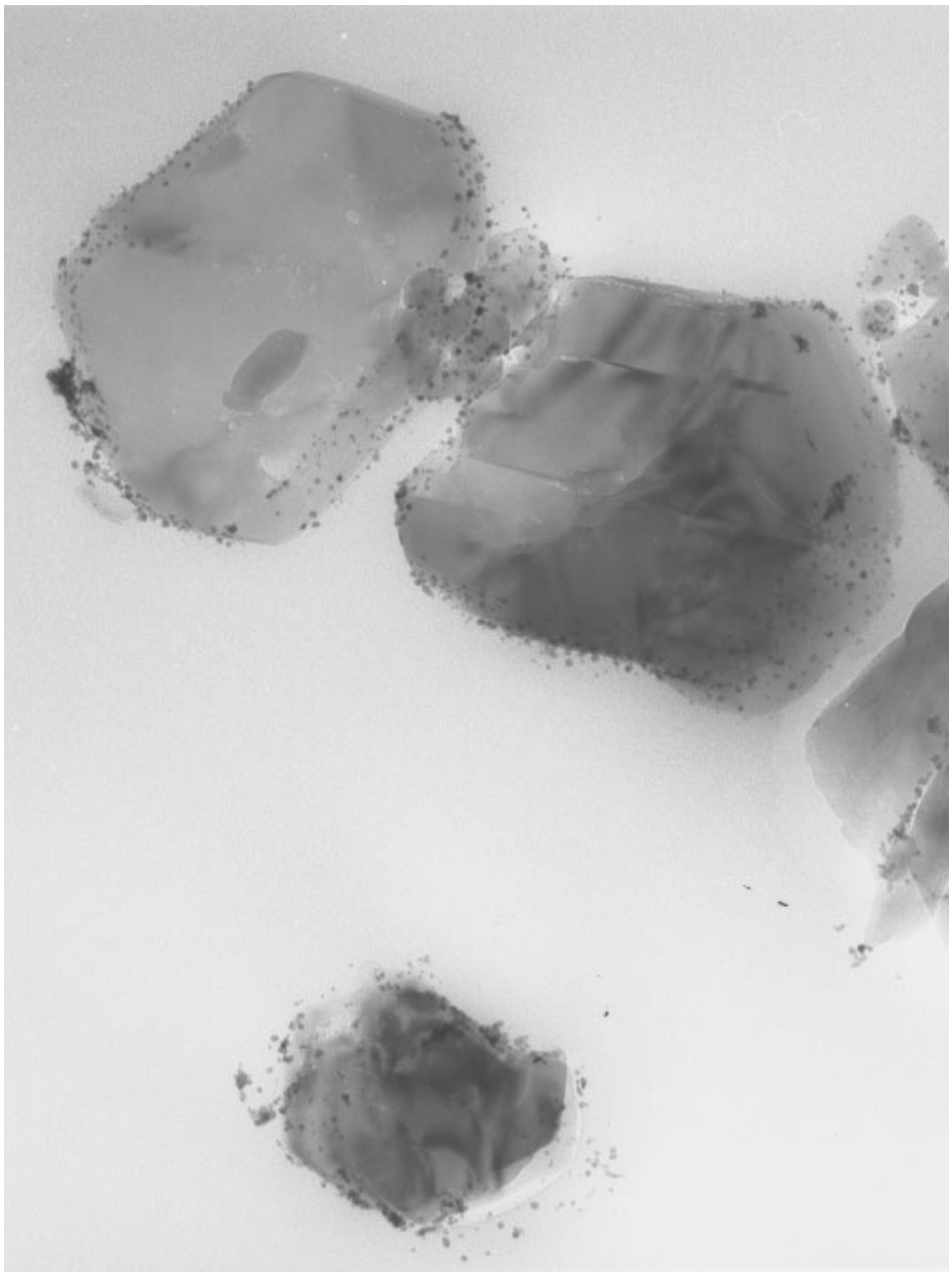

**Figure 13** TEM of a thin section of $Pd_3Pb$(SB12)/$CaCO_3$ catalyst.

 

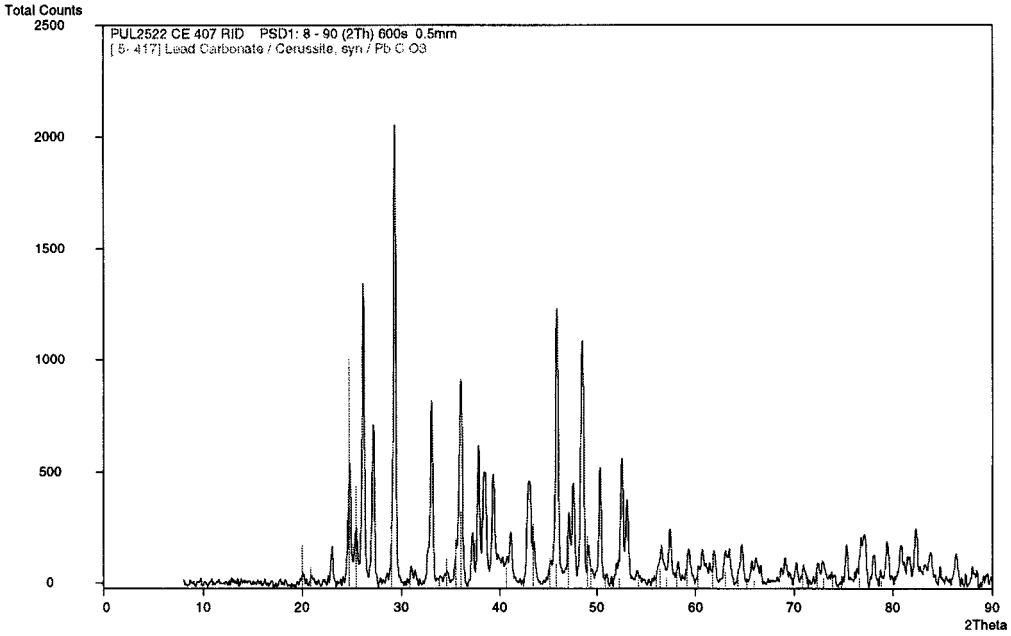


**Figure 14** XRD spectrum of the conventional Lindlar catalyst.

## Influence of the support

The Pd(SB12) colloid, which has been found to be most selective in the partial hydrogenation of 3-hexyn-1-ol, has been deposited on various supports. High weight percentages (~5% wt) of the hydrophilic colloid can be deposited on oxide supports such as alumina by simple physical adsorption. The hydrogenation activities in the cinnamic acid test were higher on $CaCO_3$ than on charcoal or the oxide supports $Al_2O_3$ and $CeO_2$ (Fig. 6).

The highest selectivity and activity in the partial hydrogenation of 3-hexyn-1-ol has been achieved on $CaCO_3$ (95%) (Fig. 7). Remarkable also is the high selectivity (94%) on $CeO_2$, but this is accompanied by a decrease in activity.

**Table 5** EDX point analysis of different positions (a–d in Fig. 16)

| Position | Detected elements | Phase |
|---|---|---|
| a | Pb | $PbCO_3$ or PbO |
| b | Ca | $CaCO_3$ |
| | O | |
| c | Pd | $Pd/CaCO_3$ |
| | Ca | |
| d | Pd | Pd |

## Bimetallic Pd/M-colloid catalysts

In the case of an SB12-stabilized colloid, the monometallic $Pd(SB12)/CaCO_3$ catalyst had a higher hydrogenation activity in the cinnamic acid test than the bimetallic $Pd/M(SB12)/CaCO_3$ catalyst (M = Rh, Ru, Ag, Cu) (Fig. 8).

In the partial hydrogenation of 3-hexyn-1-ol, a selectivity improvement has been achieved by adding 25% mol Cu, but this is accompanied by a significant loss in activity (Table 4).

## Pb-promoted catalysts

The performance of different Pb-promoted colloidal catalysts has been compared with that of conventional Lindlar catalysts (Degussa AG) having different Pb contents (3.5% wt and 0.5% wt for the partial hydrogenation of 3-hexyn-1-ol. In the case of conventional Lindlar catalysts CE 407 R/D (3.5% Pb) and Ce 407 XR/D (0.5% Pb), the selectivity increases and the activity decreases with increasing Pb content. The Pb-promoted colloidal catalysts showed increasing selectivity and decreasing activity with increasing Pb content. The $Pd(SB12)/CaCO_3$ catalyst containing 2% Pb showed the highest selectivity (98.1%), which is 0.5% higher than the conventional Lindlar catalyst containing 3.5% Pb. Additionally, this colloidal catalyst was

 

**Figure 15** TEM of $CaCO_3$.

nearly twice as fast as the conventional system, which contains 3.5% Pb (Fig. 9). The bimetallic SB12-stabilized $Pd_3Pb$ colloid supported on $CaCO_3$ had a lower selectivity (92%) compared with the monometallic system (95.3%) and also lower activity. Reducing the Pb content in the bimetallic precursor from 25% mol to 5% mol causes an enormous increase in activity and slight increase in selectivity, but both are still lower than in the case of the monometallic catalyst (Fig. 9).

TEM of the bimetallic catalyst (Fig. 10) shows that the particles are well dispersed on the support, suggesting that the low activity may well be the result of Pb surface enrichment on the colloidal particles. High-resolution TEM micro-

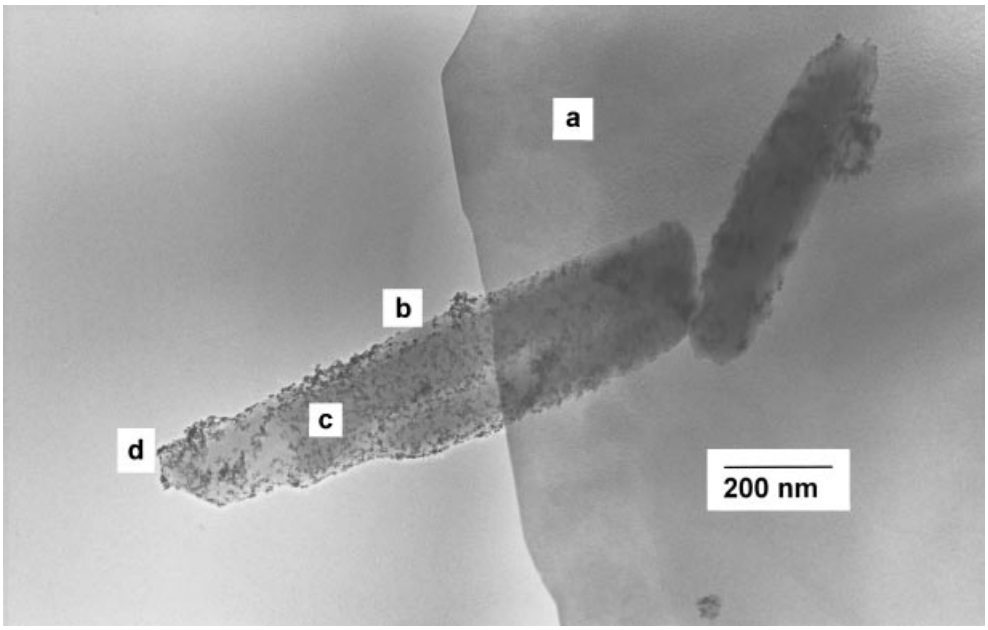


**Figure 16** TEM/EDX of the conventional Lindlar catalyst, EDX point analysis: (a) single crystals of $PbCO_3$ (no Pd particles); (b) $CaCO_3$ needles (no Pd particles); (c) Pd particles on $CaCO_3$ needles; (d) isolated Pd particles.

 

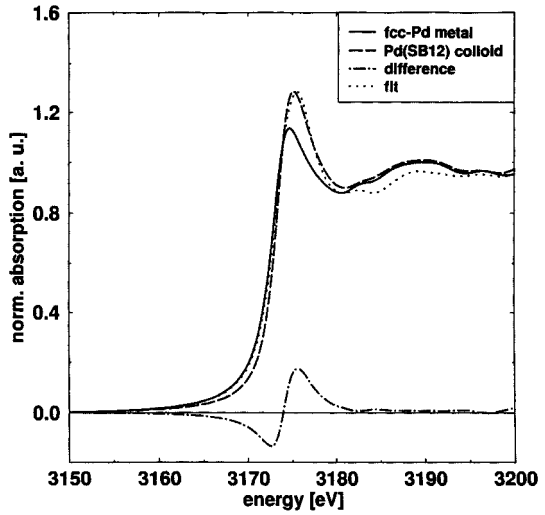


**Figure 17** Pd K-XANES of Pd(SB12) colloid and Pd powder.

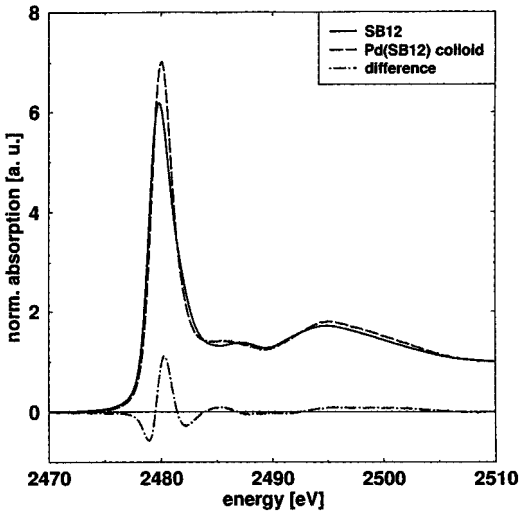


**Figure 19** S K-XANES of Pd(SB12) colloid and pure SB12.

graphs (Fig. 11) show isolated and agglomerations of three to five single particles.

EDX point analysis (Fig. 12) of several particles reveals that Pd and Pb are present in all particles with a constant Pd/Pb atomic ratio around 4:1, which is lower than the calculated value of 3:1. Probably the lower Pb concentration in the particles is caused by some unreduced $PbBr_2$, which is not alloyed with Pd (see also the XPS results).

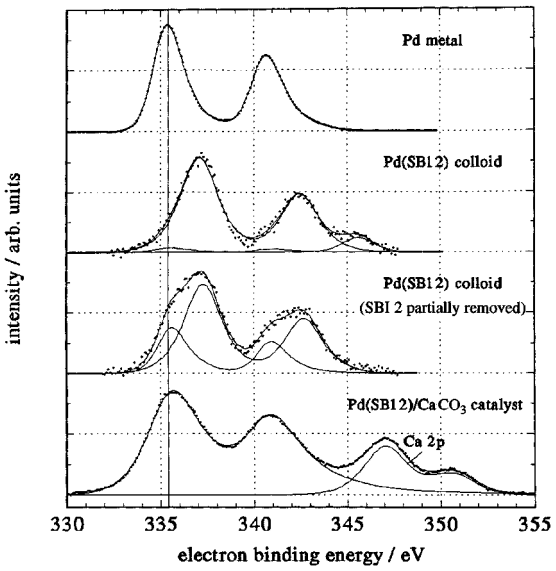


**Figure 18** Pd 3d XP spectra of Pd metal, Pd(SB12) colloid, Pd(SB12) colloid (washed) and Pd(SB12)/$CaCO_3$ catalyst.

TEM of thin sections of the catalyst (Fig. 13) shows that the colloid is adsorbed only on the surface of the support. These 'egg-shell'-type catalysts are known to be particularly well suited for selective hydrogenations. In the case of the Lindlar-type Pb-promoted catalysts, $PbCO_3$ is formed during catalyst preparation, as shown by XRD and TEM/EDX.

The XRD spectra (Fig. 14) of the Lindlar catalyst show the presence of a cerussite phase in addition to two different modifications of $CaCO_3$

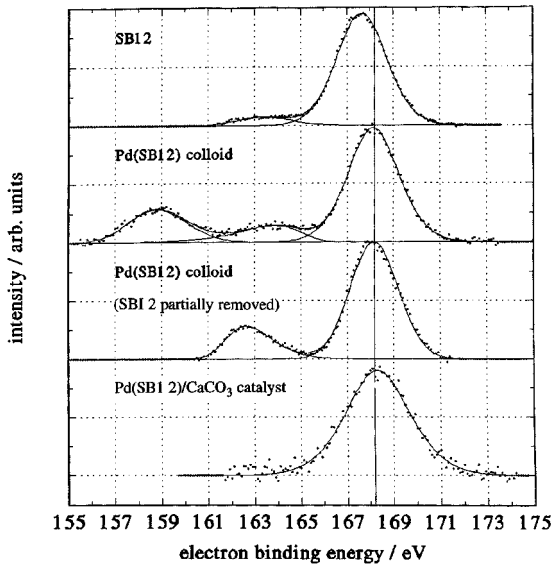


**Figure 20** S 2p XP spectra of SB12, Pd(SB12) colloid, Pd(SB12) colloid (washed and Pd(SB12)/$CaCO_3$ catalyst.

 

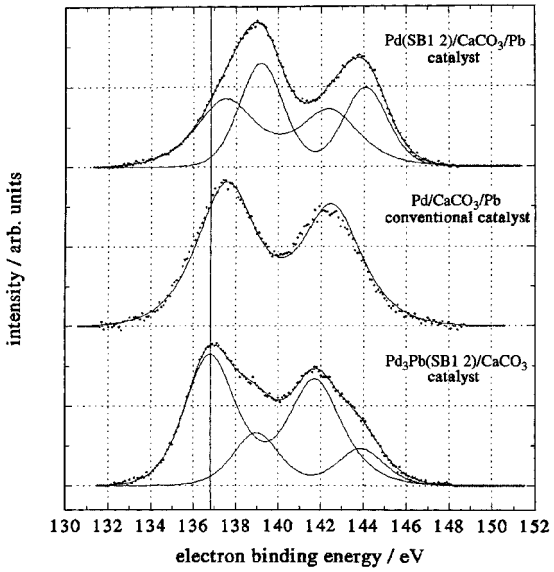


**Figure 21** Pb 4f XP spectra of Pd(SB12)/$CaCO_3$/Pb catalyst, Pd/$CaCO_3$/Pb conventional catalyst and $Pd_3Pb$(SB12)/$CaCO_3$ catalyst.

(aragonite and calcite). The Pd phase could not be detected by x-ray diffraction (XRD).

The morphology of the catalysts has been investigated by TEM/EDX. The pure $CaCO_3$ support has a needle-like morphology and consists of a mixture of aragonite and calcite (Fig. 15). In the case of the Lindlar catalyst, thin crystals of 5 μm diameter having a hexagonal symmetry (electron diffraction in the TEM) were studied by TEM (Fig. 16). EDX analysis (Fig. 16; Table 5) showed that the crystals contained Pb and O but not Ca, and they were identified as the $PbCO_3$ phase by XRD (Fig. 14). EDX analysis of the needles (Fig. 16) indicated that they were identical with the $CaCO_3$ phase. Tempering at 450 °C converted the aragonite phase completely into the calcite phase, but did not change the morphology. The Pd particles had a medium particle size of 5 nm and were situated only on the $CaCO_3$ support. EDX spot analysis of single particles (Fig. 16) revealed that some of the Pd particles contained Pb, whereas in most cases the Pb concentration in the particles lay below the detection limit.

The Pd-$L_{III}$ XANES spectrum of the Pd(SB12) colloid differs slightly in the energy position, intensity and width of the white line (Pd $2p_{3/2} \rightarrow 4d$ electronic transition) compared with Pd powder (Fig. 17). We succeeded in simulating the colloid spectrum as a superposition of the data of Pd powder (80%) and PdO (20%).[11] Since the spectra were recorded in the transmission mode and therefore the information corresponds to the total volume, a spatial differentiation of metallic and oxidized Pd is not possible. The surface-sensitive Pd 3d XP spectra of Pd powder, Pd(SB12) colloid as prepared and washed in $CH_3CN/H_2O$ (Fig. 18) were also analyzed as the superposition of two doublets (Pd $3d_{5/2}+3d_{3/2}$) representing metallic and oxidized Pd. The Pd(SB12) colloid spectrum shows that the dominating content of Pd (95% at.) is present in an oxidized state [$E$(Pd $3d_{5/2}$) = 337.2 eV] and only a minor part is metallic [$E$(Pd $3d_{5/2}$) = 335.6 eV].[12] However, it should be noted that the washing of the colloid accompanied by a loss of SB12 leads to an increase of the metallic signal intensity in the Pd 3d XP spectrum up to 30%. Support of the Pd(SB12) colloid on $CaCO_3$ led to a broad Pd 3d XPS signal centered at 335.7 eV (metallic).[12] The signal broadening in the catalyst was also observed in C 1s, S 2p, N 1s and O 1s spectra and could be explained by inhomogeneous sample charging. The influence of the protective shell seemed to have disappeared but its presence could still be detected in S 2p and N 1s detailed spectra. The Pd 3d XP spectra of Pd(SB12)/$CaCO_3$/Pb, $Pd_3Pb$(SB12)/$CaCO_3$ and the conventional Pd/$CaCO_3$/Pb catalysts (not shown) essentially remain unchanged in line shape and energy position, in comparison with the Pd(SB12)/$CaCO_3$ catalyst.

Both the XPS and XANES results point to the localization of the oxidized Pd species at the particle surface of Pd(SB12). To decide whether the interaction of the Pd particles with the protective shell is responsible for the detection of PdO-like species at the Pd particle surface, we have measured the sulfobetaine S K-XANES (Fig. 19) and S 2p-XP spectra (Fig. 20). The comparison of Pd(SB12)-colloid data with those obtained from pure SB12 yields an increasing S 2p binding energy (167.6 eV→168.2 eV) as well as a slight shift of the energy position (≈+0.5 eV) and an increasing intensity of the S K-XANES white line (S 1s→3p electronic transition) which together point to a more positive sulfur charge state in the colloid. Therefore it is probable that the interaction of the surface atoms of the Pd particles with the protective shell SB12 results in a shift in the Pd signal to the oxidized state in the XANES and

 

XP spectra.

The Pb $4f_{7/2}$; $4f_{5/2}$ XP spectrum (Fig. 21) of the Pd(SB12)/$CaCO_3$/Pb catalyst (upper spectrum) shows Pb in two different chemical states: about 50% at. of the contained Pb at *E*(Pb $4f_{7/2}$) = 138.9 eV is assigned to the educt Pb(acetate)$_2$[13] or $PbCO_3$,[14] while the other part represents PbO [*E*(Pb $4f_{7/2}$) = 137.5 eV.[15] From this chemical-state analysis the content of PbO is suggested to predominate in the conventional Pd/$CaCO_3$/Pb catalyst (Fig. 21, middle brace). A new chemical state of Pb at *E*(Pb $4f_{7/2}$) = 136.8 eV is observed in the $Pd_3Pb$(SB12)/$CaCO_3$ catalyst (Fig. 21, lower spectrum); because of the similarity of this value to that for metallic Pb,[15] this signal is assigned to the $Pd_3Pb$ alloy. A residual content (≈25% at.) of the educt $PbBr_2$ is detected at *E*(Pb $4f_{7/2}$) = 138.8 eV.[15]

*Acknowledgements* This work was supported by the BMBF (German Ministry of Education, Science, Research and Technology) (FKZ 03 D0007 A2). We thank Dr A. Freund and Dr E. Auer (Degussa AG) for valuable discussions, supplying the catalysts and various supports, and measurement of the thin-section TEM (Fig. 12). We are grateful to Dr B. Tesche and Dipl. Ing. B. Spliethoff (Max-Planck-Institut für Kohlenforschung) for the TEM/EDX analyses (Figs 11, 14, 15) and to Dr K. Seevogel (Max-Planck-Institut für Kohlenforschung) for IR investigations.

## REFERENCES

1. L. P. Somogyi, *Chem. Ind. (London)* 170 (4 March 1996).
2. E. N. Marvell and T. Li, *Synthesis* 457 (1973).
3. C. Paal and H. Schiedewitz, *Ber. Dtsch. Chem. Ges.* **63** 766 (1930).
4. H. Lindlar, *Helv. Chim. Acta* **35**, 447 (1952).
5. J. G. Ulan, E. Kuo, W. F. Maier, R. S. Rai and G. Thomas, *J. Org. Chem.* **52**, 3126 (1987).
6. W. Palczewska, A. Jablonski, Z. Kaszkur, G. Zuba and J. Wernisch, *J. Mol. Catal.* **25**, 307 (1984).
7. H. Bönnemann, W. Brijoux, R. Brinkmann, R. Fretzen, T. Joußen, R. Köppler, B. Korall, P. Neiteler and J. Richter, *J. Mol. Catal.* **86**, 129 (1994).
8. H. Bönnemann, R. Brinkmann and P. Neiteler, *Appl. Organomet. Chem.* **8**, 361 (1994).
9. T. S. Ertel, H. Bertagnolli, S. Hückmann, U. Kolb and D. Peter, *Appl. Spectrosc.* **46**(4), 690 (1992).
10. H. Bönnemann, G. Braun, W. Brijoux, R. Brinkmann, A. Schulze-Tilling, K. Seevogel and K. Siepen, *J. Organomet. Chem.* **520**, 143 (1996).
11. J. Rothe, PhD Thesis, Bonn University, 1996.
12. C. D. Wagner, W. M. Riggs, L. E. Davis, J. F. Moulder and G. E. Muilenberg, *Handbook of X-ray Photoelectron Spectroscopy*, Perkin-Elmer Corp., Eden Prairie, 1975.
13. V. I. Nefedov, Y. V. Salyn and X. Keller, *Zh. Neorg. Khim.* **24**, 2564 (1979).
14. J. A. Taylor, *J. Vac. Sci. Technol.* A2, 771 (1984).
15. L. R. Pederson, *J. Electron Spectrosc. Relat. Phenom.* **28**, 203 (1982).

 